Modulation of ENSO-Based Long-Lead Outlooks of Southwestern U.S. Winter Precipitation by the Pacific Decadal Oscillation

DAVID S. GUTZLER

Department of Earth and Planetary Sciences, University of New Mexico, Albuquerque, New Mexico

DEIRDRE M. KANN

National Weather Service, Albuquerque, New Mexico

CASEY THORNBRUGH

Department of Earth and Planetary Sciences, University of New Mexico, Albuquerque, New Mexico

(Manuscript received 20 December 2001, in final form 21 June 2002)

ABSTRACT

Seasonal predictability of winter precipitation anomalies across the U.S. Southwest derived from knowledge of antecedent, late-summer Pacific Ocean surface temperatures is examined empirically. Previous studies have shown that equatorial Pacific SST anomalies associated with the El Niño–Southern Oscillation (ENSO) cycle, which are persistent from late summer through winter, exhibit a strong relationship with winter precipitation in Arizona and New Mexico. Here the degree to which seasonal predictability in this region is modulated by longer-term oceanic fluctuations associated with the Pacific decadal oscillation (PDO) is assessed. When all years from 1950 through 1997 are considered as a single dataset, inclusion of the PDO signal adds only slightly to the ENSO-based statistical predictability of Southwest winter precipitation anomalies. However, when the dataset is split into two subperiods delineated by a major shift in the PDO (before and after 1977), the ENSO-based predictability and, to a lesser extent, PDO-based predictability are substantially modified. Before 1977, negative winter precipitation anomalies are strongly tied to ENSO cold years but warm years do not systematically lead to positive precipitation anomalies. After 1977, this asymmetry is reversed and positive precipitation anomalies predictably follow warm ENSO years but cold years yield no precipitation predictability. Within each subperiod, interannual PDO fluctuations yield less predictability than ENSO fluctuations. Thus ENSO-based predictability seems to undergo a profound decadal modification that might be associated statistically with the PDO, but the physical link to North Pacific Ocean temperatures is problematic.

1. Introduction

A large fraction of current operational seasonal predictability across North America is derived from knowledge of the state of the El Niño–Southern Oscillation (ENSO) cycle (Trenberth 1997). Across the southwestern United States, winter and spring precipitation anomalies are positively correlated with central and eastern equatorial Pacific Ocean surface temperatures. The Southwest is anomalously wet during the winter and spring seasons following El Niño, when the Tahiti–Darwin Southern Oscillation index (SOI) is negative, and anomalously dry following La Niña, when the SOI is positive (Redmond and Koch 1991). This relationship has been established observationally for more than a decade (Ropelewski and Halpert 1986, 1987). The correlation is particularly pronounced using spring streamflow data that effectively integrate high-elevation snowpack over the entire cold season (Cayan and Webb 1992). The ENSO–Southwest precipitation correlation is now routinely considered each year by the National Oceanic and Atmospheric Administration (NOAA) Climate Prediction Center and other climate forecast centers when long-lead winter outlooks are prepared.

The ENSO cycle is closely, though not perfectly, phase-locked to the seasonal cycle in the tropical Pacific, such that by late boreal summer each year it is usually apparent whether the equatorial Pacific is moving toward an ENSO extremum (either cold or warm) the following boreal winter (Rasmusson and Carpenter 1982; Wallace et al. 1998). Midlatitude teleconnections forced by atmospheric heating anomalies associated with tropical rainfall anomalies are also most pronounced in the boreal winter season (Trenberth et al. 1998). Thus the seasonality of both the ENSO cycle and

Corresponding author address: Dr. David S. Gutzler, Earth and Planetary Sciences Dept., University of New Mexico, Albuquerque, NM 87131-11116.
E-mail: gutzler@unm.edu

of tropical–extratropical teleconnection dynamics acts to create a winter seasonal maximum in ENSO-based long-lead predictability of North American climate anomalies.

Longer-term fluctuations of Pacific Ocean temperatures and North American precipitation have been scrutinized more recently (Graham 1994; Latif and Barnett 1994, 1996). Mantua et al. (1997) described a low-frequency mode of Pacific Ocean variability centered off the equator in the Northern Hemisphere the spectrum of which contains more power at decadal periods than the ENSO signal. This Pacific decadal oscillation (PDO, as it shall be denoted in this paper) apparently is correlated with oceanic conditions near the North American coast (Bernal et al. 2001) and with precipitation across the southwestern United States (Gershunov and Barnett 1998; Higgins et al. 2000; Liles 2000) and northwestern Mexico (Brito-Castillo et al. 2002).

Higgins et al. (2000) present maps showing that PDO-like variability (which they called ''tropical interdecadal'' fluctuations) accounts for at least as much interannual precipitation variance across the southwestern United States as a higher-frequency interannual ENSO-related index. Barlow et al. (2001) reached similar conclusions for summer-season hydroclimatic variability. McCabe and Dettinger (1999) showed pronounced decadal variations in interannual correlations between ENSO-related indices, especially the Tahiti–Darwin Southern Oscillation index, and winter precipitation across western North America. They related these decadal variations to the PDO.

A goal of this study is to quantify the extent to which prediction schemes incorporating both ENSO and PDO indices might enhance the statistical relationship between Pacific SST and southwestern U.S. precipitation. Covariate relationships with a season of lead time [SST leading precipitation, as carried out in the analysis by Redmond and Koch (1991)] that may have practical predictive value are established to determine whether additional information available in late summer pertaining to the state of the PDO significantly modifies or enhances the ENSO-based predictability of Southwest winter precipitation anomalies.

Gershunov and Barnett (1998) calculated composites of the seasonal frequency of heavy precipitation across the United States with respect to ENSO extrema separately for high and low North Pacific SST years [their North Pacific oscillation (NPO) index is similar to the Mantua et al. (1997) PDO index]. They concluded that the ENSO signal in wintertime North American climate anomalies is significantly enhanced when the PDO and ENSO constructively interfere (El Niño + high PDO, La Niña + low PDO) and is diminished when PDO and ENSO destructively interfere.

This study extends the Gershunov and Barnett (1998) and McCabe and Dettinger (1999) analyses by considering in detail a region of the United States with a well-known high-amplitude ENSO winter climate signal. Results are expressed using a statistical framework similar to operational long-lead outlooks. The first issue addressed is the relative importance of ENSO and PDO indices as individual predictors of Southwest precipitation anomalies. This is followed by an examination of multivariate predictability incorporating information from both ENSO- and PDO-related conditions in the Pacific. The ultimate goal is to inquire whether some practical enhancement of seasonal predictability of Southwest precipitation is possible.

2. Data and analysis procedure

a. Pacific SST time series

The Niño-3 SST index averaged over three late summer months (July–September, JAS) is used as the ENSO-associated predictor of southwestern U.S. precipitation anomalies for the subsequent winter (December–March, DJFM). The period of study extends from 1950 through the winter of 1997/98, or 48 yr. Niño-3 is an average of ocean surface temperature within 5° of the equator between 150° and 90°W, compiled and disseminated by the NOAA Climate Prediction Center (obtained online at ftp.ncep.noaa.gov/pub/cpc/wd52dg/data/indices). Large positive values of Niño-3 are associated with El Niño, and large negative values are associated with La Niña. The solid and open squares on the solid curve in Fig. 1a mark the highest and lowest tercile values of Niño-3 (i.e., warmest 16 yr and coldest 16 yr of the 48-yr record). It should be noted that the upper- and lower-tercile values include several more years than are typically considered ''extreme events'' by ENSO analysts; however, considering ENSO terciles expands the sample size of warm and cold event years in our half-century data record.

In operational practice, winter-season outlooks issued in the autumn are based on dynamical predictions of ENSO conditions, not just persistence of JAS conditions as assumed in this study. However, as mentioned above, persistence of JAS Niño-3 anomalies provides an excellent qualitative predictor of ENSO through the boreal winter season: the seasonal lag correlation between JAS and subsequent DJF Niño-3 values is 0.86.

The Mantua et al. (1997) PDO index is used in this study to characterize Pacific low-frequency variability. Mantua et al. (1997) derived their index from an EOF analysis of North Pacific SST (available online at time of writing from the University of Washington at http://tao.atmos.washington.edu/pdo/). Positive values of this index describe anomalously cold SST anomalies around 45°N. North Pacific SST anomalies are statistically associated with warm anomalies in the Niño-3 region (Weare et al. 1976; Mantua et al. 1997) so ENSO and the Mantua et al. PDO are not completely independent fluctuations. Seasonal values of the PDO are in fact highly correlated with ENSO indices such as Niño-3 (Zhang et al. 1997; Thornbrugh et al. 2001).

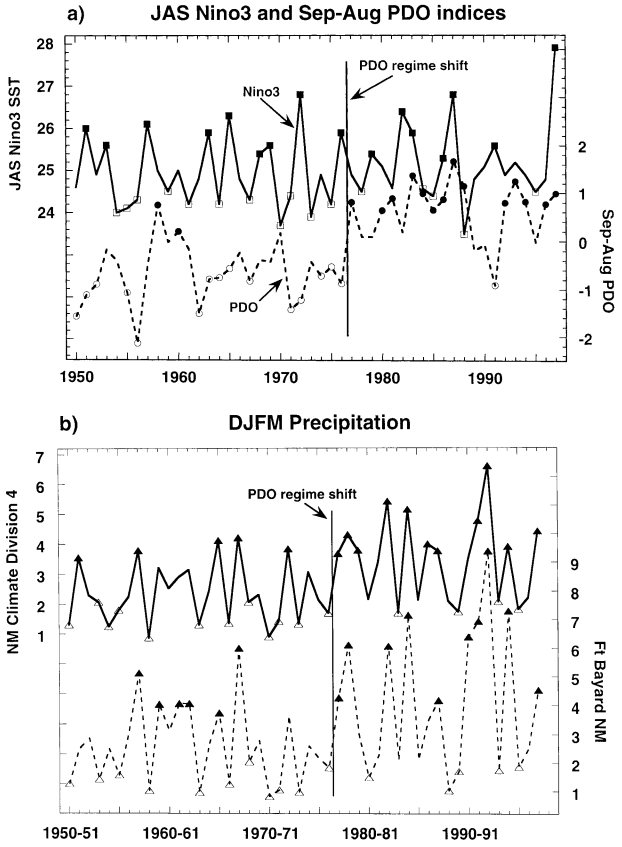

FIG. 1. (a) Annual values of JAS Niño-3 SST (solid line; °C) and nondimensional Sep–Aug PDO index (dashed line) for 1950–97; years of PDO index correspond to the summer months (e.g., Sep 1950–Aug 1951 average is plotted as 1951). Solid squares and open squares mark annual values in the upper and lower terciles of the 48-yr sample of Niño-3. Solid and open circles mark upper- and lower-tercile PDO values. (b) Annual values of DJFM precipitation averaged over climate division 4 (the Southwest Mountains division) in NM (solid line; in.), and at Fort Bayard, NM, (dashed line) for 1950/51–1997/98 period. Solid and open triangles mark values in the upper and lower terciles of the 48-yr period of record as in (a).

It is important to note that other ENSO and PDO indices could have been chosen for this study. The ENSO cycle is described by oceanic and atmospheric indices, all of which are significantly but imperfectly correlated (e.g., Deser and Wallace 1987) in ways that could have some effect on predictability statistics (Redmond and Koch 1991). The PDO is even less definitively described than ENSO. As discussed in section 1, researchers have created different PDO-like indices, and there is currently no clear consensus on the index that best characterizes Pacific decadal variability.

Because the emphasis in this study is on the decade-scale variations of PDO, annual averages of the Mantua et al. monthly index using a September–August averaging period were calculated. As depicted in Fig. 1a, year-to-year fluctuations of this annual PDO index are not highly correlated with late-summer (JAS) Niño-3 fluctuations. The linear correlation between the two time series in Fig. 1a is just 0.13, and only 4 of the warmest 16 Niño-3 values (solid squares) and highest 15 PDO values (solid circles) are coincident.[1]

As documented by Mantua et al. (1997) and evident in Fig. 1a, the PDO contains more decade-scale variability than do equatorial ENSO indices such as Niño-3. Over the last half-century, the PDO exhibits decadal variability that could be described either as an upward trend or as a regime shift in the late 1970s toward more positive values, that is, warmer water on the equator and cooler water in the North Pacific. The upward trend/shift in PDO is very pronounced, so that 15 of 16 (94%) lower-tercile values (open circles) occur before 1977 and 14 of 15 (93%) upper-tercile values occur after 1976 (note that 27 of the 48 yr of data, or 56%, occur before 1977 and 21 yr, or 44%, occur after 1977). Gershunov and Barnett (1998) found a similarly strong difference before and after 1977 in their decadal Pacific index (NPO in their nomenclature), and Higgins et al. (2000) illustrate a pronounced change in their tropical interdecadal index at about this same time. We will refer to the climate change in 1977 as the PDO regime shift.

Decadal changes in Niño-3 over this period of record are smaller, although there is a hint in Fig. 1a that Niño-3 temperatures rose during the last several decades [upward equatorial Pacific temperature trends are more pronounced west of the date line (Gutzler 1996)]. The upper- and lower-tercile years are much more evenly distributed across the period of record in the Niño-3 record relative to PDO: 11 of 16 lower-tercile years (69%) occur before 1977 and 7 of 16 upper-tercile years (44%) occur after 1977.

b. Statistical predictability of winter precipitation

The objective of this study is to consider the predictive value of the two time series shown in Fig. 1a for southwestern U.S. precipitation the following winter. Precipitation records are obtained from National Weather Service and cooperative observer stations throughout New Mexico and Arizona. Most of the calculations were based on spatial averages of these data (climate divisions) derived by the NOAA National Climatic Data Center. Monthly precipitation totals were summed over the four months between December and March each boreal winter season.

The time series of DJFM precipitation in New Mexico division 4 (NM4), the ''Southwest Mountains'' division, is shown in Fig. 1b. As in Fig. 1a, the 48 seasonal values are divided into terciles, and the upper- and lower-tercile values are marked on the plot. Like the PDO time series in Fig. 1a, most of the lower-tercile values occur in the

[1] There is a large gap in the 48-yr sample of PDO values between the 15th and 16th ranked values (0.64 and 0.20), forming a logical boundary. Thus the upper PDO tercile defined for this study contains 15 annual values and the medial tercile contains 17 values, rather than 16 each.

early decades of the dataset (12 of 16 prior to 1977), and most of the upper-tercile values occur late in the dataset (11 of 16 after 1977).

There are inherent inhomogeneities in climate-division averages associated with the time-varying distribution of station data within each division. To alleviate concerns that an increase in divisional precipitation over the second half of the twentieth century is an artifact of such inhomogeneities, a small sample of individual station records was examined. The DJFM precipitation time series for a station located in NM4, Fort Bayard, is also shown in Fig. 1b. The Fort Bayard time series exhibits the same general character, including the upward trend (or shift) in winter precipitation late in the period of record, as the divisional time series. The correlation between the NM4 and Fort Bayard time series in Fig. 1b is 0.89; most, but not all, of the upper- and lower-tercile years are the same in the two records.

Scatterplots (discussed in section 3) were used to evaluate the predictive skill for DJFM precipitation derived from prior knowledge of SST in the Pacific. The fraction of years with anomalous Niño-3 or PDO indices in late summer that are followed by anomalous winter precipitation was determined using the scatterplots. The a priori hypothesis based on previous studies is that upper-tercile Niño-3 or PDO values should systematically lead to upper-tercile precipitation anomalies and lower-tercile SST indices should lead to lower-tercile precipitation anomalies.

Results have been reproduced using slightly different combinations of late-summer SST predictor and winter/spring precipitation predictand periods, including August–October Niño-3 predictors and DJF or JFM precipitation predictands. The results and interpretation that follow are not sensitive to the particular choices of predictor/predictand periods. The key results were also reproducible using scatterplots derived from station data such as the Fort Bayard data shown in Fig. 1b instead of climate-division data.

c. Assessment of seasonal predictive skill

Assessment of predictive skill is carried out using a modified Brier score. For a particular location and subset of N winters (e.g., all the winters following upper-tercile Niño-3 values) the distribution of precipitation anomalies can be represented as $x/y/z$, where x is the number of winters with dry (lower tercile) precipitation anomalies, y is the number of near-normal (medial tercile) anomalies, z is the number of wet (upper tercile) anomalies, and $x + y + z = N$. The hypothesis in this case is that warm Niño-3 values should be followed by wet winters; if this relationship were perfect, the winter precipitation anomaly distribution would be $x/y/z = 0/0/N$. On the other hand, if Niño-3 has no effect on subsequent winter precipitation, then the expected tercile distribution would be even, that is, $a/a/a$, where $a = N/3$.

To define predictive skill, the observed distribution $x/y/z$ is scored by assigning a value of 0 to each correct forecast or ''hit,'' a value of 1 to each winter in which the observed precipitation anomaly is one tercile away from the predicted tercile (i.e., the observed medial anomalies), and a value of 2 to each winter in which the observation is two terciles away from the forecast (i.e., completely wrong: in this example, lower-tercile precipitation anomalies). So, for distributions of wet winter predictions (following positive Niño-3 or PDO values), the skill score is simply

$$S_+ = (2x + y)/N \tag{1a}$$

and similarly, for dry winter predictions following negative Niño-3 or PDO values,

$$S_- = (y + 2z)/N. \tag{1b}$$

This metric differs from a standard Brier score (Wilks 1995) because the errors associated with nonhits are not squared (a two-category error in S_+ or S_- counts as 2, not 4). Equations (1a) and (1b) have the convenient property that a climatological distribution $a/a/a$, which represents a null hypothesis for predictive skill, generates a skill score of S_- or $S_+ = 1$. A set of perfect seasonal forecasts, with distributions of $0/0/N$ or $N/0/0$, generates a skill score of $S_+ = 0$ or $S_- = 0$, respectively. Thus, skill scores of less than 1 are generated by an observed anomaly distribution skewed toward the predicted tercile, indicating some level of predictive skill exceeding ''climatology.'' Scores equal to or greater than 1 indicate no skill.

3. ENSO, PDO, and Southwest winter precipitation

Scatterplots were constructed for all climate divisions in New Mexico and Arizona. The plot for NM4 is shown in Fig. 2 as an example. The headwaters of the Gila River, whose spring streamflow anomalies are highly correlated with ENSO fluctuations (Molles and Dahm 1990), are located within NM4. The x coordinate of each point is its JAS Niño-3 value for a particular year, and the y coordinate is the corresponding September–August PDO index. The subsequent DJFM precipitation anomaly is represented by the symbol plotted for each year, divided into terciles. An $\times$ represents a precipitation anomaly in the medial tercile (i.e., near-climatological precipitation). An open circle denotes a negative (dry) precipitation anomaly, in the lowest tercile of the 48 yr, with the larger circles denoting dry anomalies in the lower half of the dry tercile (i.e., an extreme negative anomaly). Solid dots denote positive (wet) precipitation anomalies in the same way, with the larger dots representing the wettest 1/6 of the DJFM values.

The vertical lines in Fig. 2 split the 48 yr of data into Niño-3 terciles corresponding to the extrema marked by the solid and open squares in Fig. 1a. The trio of numbers 5/1/10 to the right of the x-axis label indicates the distribution of dry/medial/wet DJFM seasons in NM4

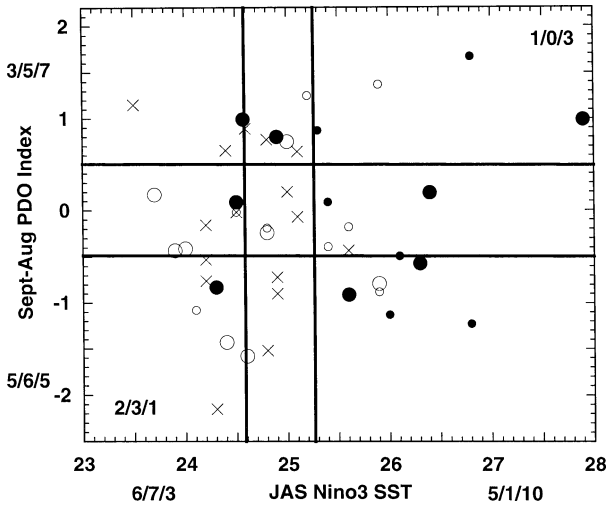

FIG. 2. Scatterplot of DJFM precipitation in NM4 plotted against antecedent JAS Niño-3 SST and Sep–Aug PDO values. Solid circles denote precipitation values in the highest tercile (larger circles for the highest sextile, smaller circles for the second sextile), and open circles similarly denote precipitation values in the lowest tercile. See text for explanation of the trios of numbers surrounding each axis label and within the plot.

following upper-tercile (warm) values of JAS Niño-3 SST. Using the definitions introduced in section 2c, $x/y/z = 5/1/10$, $N = 16$, and $S_+ = 0.69$.

The fraction of wet winters following warm Niño-3 is $z/N = 0.62$, which exceeds the fraction expected by chance (0.33) by 0.29 or 29% (of N). Following the convention employed by the National Centers for Environmental Prediction (NCEP) in its operational long-lead outlook maps, +29 would be the numerical value assigned to this region for a winter long-lead outlook issued in October when Niño-3 is warm. Enhanced probabilities exceeding 20 are unusual on NCEP's operational long-lead outlooks, demonstrating the historically strong El Niño effect on winter precipitation in the NM4 climate division.

The corresponding distribution of winter precipitation anomalies following cold JAS Niño-3 (also shown on the x-axis label) is 6/7/3, yielding a skill score of $S_- = 0.81$. The observed chance of a dry winter following cold Niño-3 is 6/16 (0.37), exceeding the null hypothesis of 0.33 by only 4%. On an NCEP long-lead outlook map, this value, less than +5, would be insufficient to plot, and (unless other long-lead forecast tools indicate otherwise) this region would be labeled CL, meaning that there is little or no basis for a long-lead outlook different from climatology, based just on Niño-3.

The horizontal lines in Fig. 2 split the data into terciles based on the preceding September–August PDO index. The trios of numbers just above and below the y-axis label show the distributions of NM4 winter precipitation anomalies following negative or positive August–September PDO years. Negative PDO yields no predictive skill at all (5/6/5 yields $S_- = 1.0$ with no enhanced probability of a dry winter).

The corresponding precipitation outlook for positive PDO yields an observed distribution of 3/5/7, so $S_+ = 0.73$ and the enhanced probability of a wet winter is +13 (7/15 = 46.7%, about 13% higher than the 33% climatological expectation). The S_+ metric indicates that positive PDO generates slightly less seasonal predictive skill of NM4 winter precipitation than does warm Niño-3.

The trios of numbers just within the upper-right and lower-left corners of the scatterplot illustrate multivariate predictions, based on both SST predictors exhibiting lower- or upper-tercile anomalies. The seasonal predictability implied using both ENSO and PDO predictors is obtained by examining the data points in the upper-right or lower-left corners of the plot. The set of four warm Niño-3 + PDO years (upper right) yields a precipitation anomaly distribution of 1/0/3, so $S_+ = 0.5$ and the fraction of wet winters is enhanced by 42% over the climatological probability of 33%, but that result is based on a very small sample. The multivariate prediction yielded by lower-tercile values of both Niño-3 and PDO is 2/3/1 (lower right), so $S_- = 0.83$, which in this case is little different from random chance.

Scatterplots like Fig. 2 were calculated for each climate division in Arizona and New Mexico. Comparison of the NCEP-style enhanced probabilities with plots with S_- and S_+ values gives us a sense of how to interpret the skill scores. By construction, S scores of 1 or more demonstrate no skill at all relative to climatology. Values greater than about 0.9 are so slightly skewed that no operationally useful predictability is indicated. The S values between about 0.75 and 0.9, derived from sample sizes larger than the multivariate predictions described above, indicate modestly meaningful predictive skill. Values between 0.6 and 0.75, or smaller, come from distributions that are markedly skewed toward the predicted tercile.

Skill scores for all Arizona and New Mexico climate divisions are illustrated separately for cold or warm Niño-3 predictors and negative or positive PDO predictors. On the Niño-3-based maps (Fig. 3), all divisions except Arizona division 4 exhibit some useful predictability for both cold and warm years. Seasonal predictability is generally somewhat higher (lower S scores) for warm events leading wet winters (Fig. 3b) than for cold events leading dry winters (Fig. 3a). Skill scores based on cold Niño-3 years (Fig. 3a) are mostly in the range of very modest predictability. Somewhat lower S scores are associated with wet winters following warm Niño-3 seasons (Fig. 3b), with enhanced precipitation probabilities of greater than 20% in five divisions scattered around the two states.

The corresponding S scores derived from PDO terciles are mapped in Fig. 4. Like the NM4 example, S scores across Arizona and New Mexico are broadly comparable to, or somewhat higher than, the Niño-3-based scores. Five of the 15 divisions in Arizona and

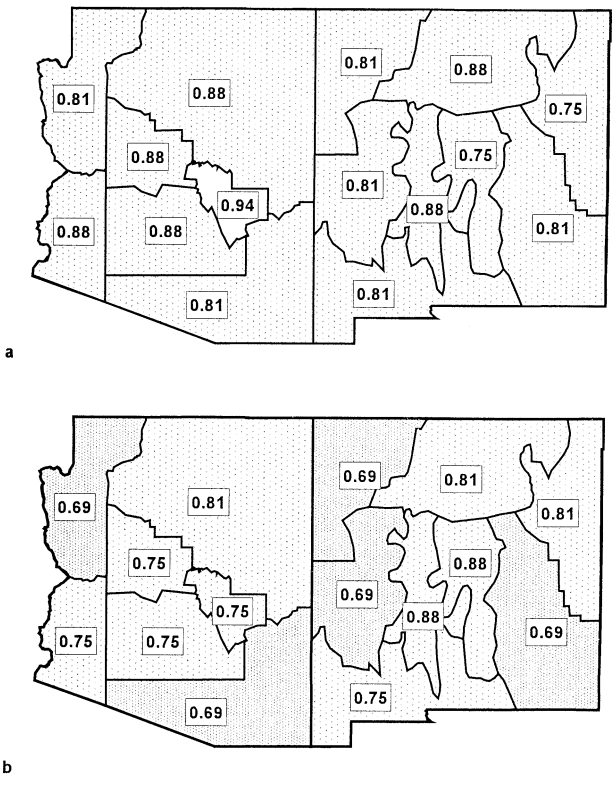

FIG. 3. Skill-score maps for climate divisions in AZ and NM. (a) Map of skill-score S_- associated with predictions of lower-tercile (dry) DJFM precipitation anomalies following cold JAS Niño-3 SST anomalies, derived from the 16 lower-tercile Niño-3 values (open squares in Fig. 1a). Intensity of map pattern corresponds to decreasing S score: $S \geq 0.90$, blank; $0.75 \leq S < 0.90$, lightly stippled; $0.60 \leq S < 0.75$, stippled; $0.45 \leq S < 0.60$, vertically striped; and $S < 0.45$, heavily stippled. (b) As in (a) but for skill score S_+ associated with predicting upper-tercile (wet) DJFM precipitation anomalies following warm JAS Niño-3 SST anomalies, derived from the 16 upper-tercile Niño-3 values (solid squares in Fig. 1a).

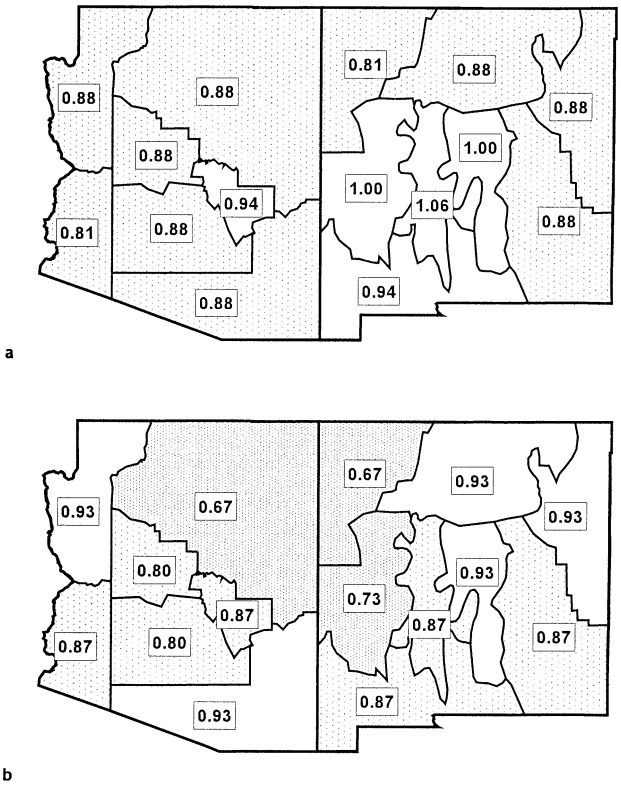

FIG. 4. (a) As in Fig. 3a but using lower-tercile values of Sep–Aug PDO values as the predictor (open circles in Fig. 1a). (b) As in Fig. 3b but using upper-tercile values of Sep–Aug PDO values as the predictor (solid circles in Fig. 1a).

New Mexico exhibit S_- scores greater than 0.9, indicative of no predictive skill during cold/negative years. Like the Niño-3-based results, positive PDO anomalies provide more predictive skill than do negative PDO anomalies. With these results, it can be concluded that Niño-3 is a slightly better overall seasonal predictor than PDO for wintertime southwestern U.S. precipitation anomalies. This conclusion is different from results presented by Gershunov and Barnett (1998), who show distinctly more anomalous frequencies of heavy precipitation associated with La Niña (cold Niño-3) than with El Niño (warm Niño-3).

Multivariate S scores and enhanced probabilities, such as those discussed for NM4 in Fig. 2, were examined for each division but are not shown. As was the case for NM4, in the divisions with the lowest warm Niño-3-based S scores, addition of the PDO generally increases statistical predictability slightly. There is no corresponding enhancement of forecast skill derived from multivariate prediction incorporating cold Niño-3 and negative PDO.

However, as the NM4 scatterplot exemplifies, the sample size of the multivariate prediction is small, and so the robustness of this result is uncertain. Equally important from an operational perspective, the very small sample size indicates that such a multivariate prediction cannot be made in most years (i.e., years of coincident ENSO and PDO extrema are uncommon). Thus the multivariate predictions of winter precipitation based on simultaneous PDO and Niño-3 anomalies, derived from historical records, are probably not useful operationally.

4. Modulation of seasonal predictability by the 1970s regime shift

The results described in the previous section suggest that, considered separately, the Niño-3 and PDO indices have similar effects on seasonal predictability of winter precipitation in the Southwest, with Niño-3 providing considerably more predictive skill. In this section, a different approach to constructing predictability scatterplots is defined that clarifies the effect of the PDO. The data are explicitly separated into subperiods before and after the PDO regime shift in 1977. This year rep-

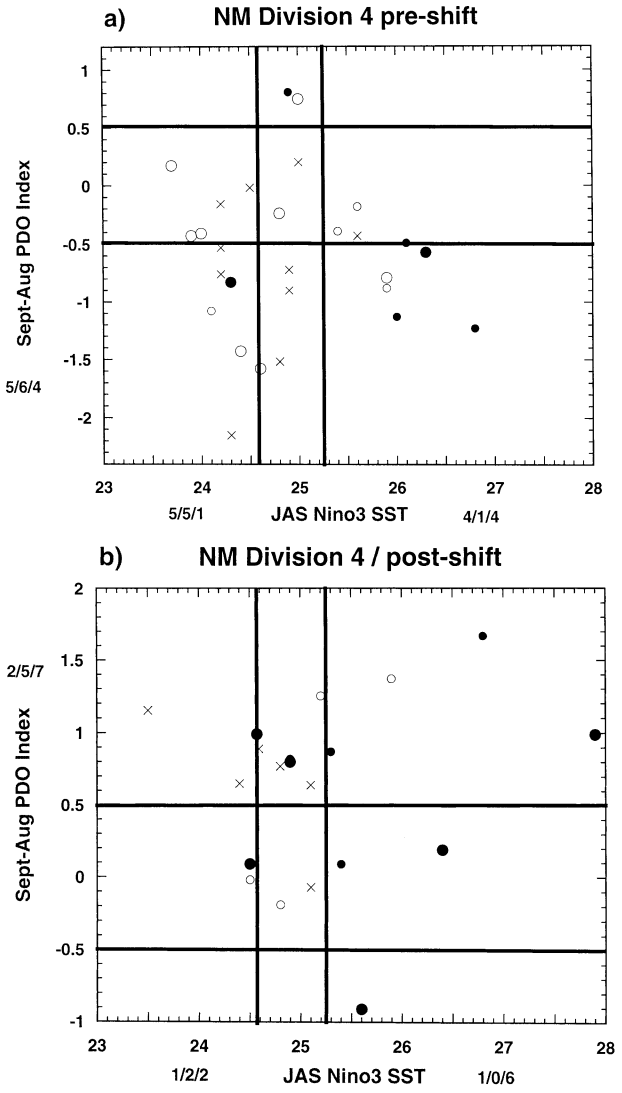

FIG. 5. (a) Scatterplot of DJFM precipitation in NM4 as in Fig. 2 but based on just the 27 yr of data (1950–76) preceding the PDO regime shift shown in Fig. 1a. (b) As in (a) but based on just the 21 yr of data (1977–97) after the PDO regime shift.

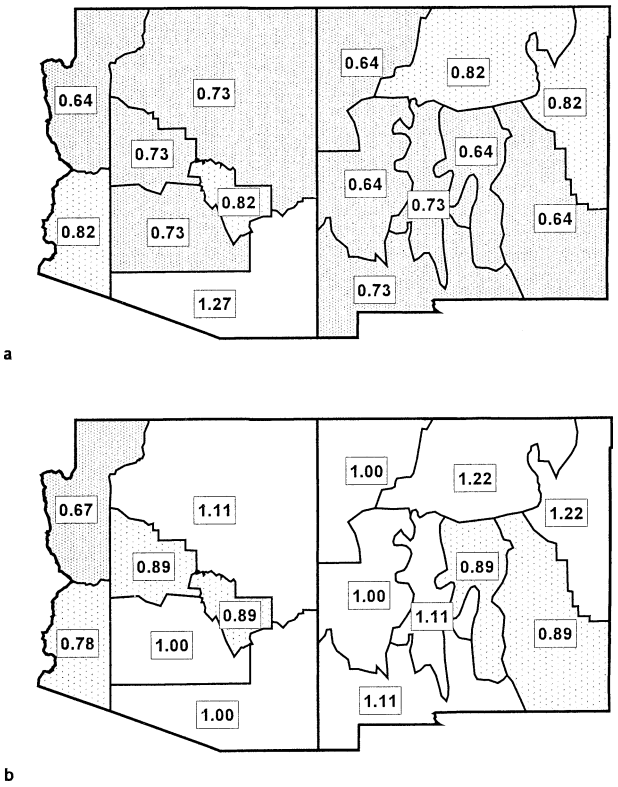

FIG. 6. Skill-score maps based on (a) cold and (b) warm Niño-3 temperatures, as in Fig. 3, but based only on years prior to the 1977 PDO regime shift shown in Fig. 1a.

resents the only major shift described by Gershunov and Barnett (1998) in their twentieth-century NPO time series manifested in the 1950–97 data record; another mid-century shift in their record occurred in 1947, a few years prior to the start of our record.

Predictability scatterplots for NM4 for the 1950–76 and 1977–97 predictor periods are shown in Fig. 5. These plots collectively depict the same data points shown in Fig. 2 but now separated by the 1977 PDO regime shift. The upper- and lower-tercile limits of Niño-3 and PDO derived from the full period of record are maintained, with the result that there is only one upper-tercile PDO year in the 1950–76 data (Figs. 1a and 5a) and one lower-tercile PDO year in the 1977–97 data (Figs. 1b and 5b).

There is a pronounced difference in ENSO-based predictability before and after the regime shift. In the pre-shift data subset (Fig. 5a) cold Niño-3 values systematically lead to a highly skewed distribution of NM4 winter precipitation: the cold Niño-3-based precipitation tercile values are 5/5/1, yielding a skill score $S_- = 0.64$ and an enhanced predictability of a dry winter of 12%. Warm Niño-3 values, however, lead to a precipitation tercile distribution of 4/1/4, generating no significant predictability of NM4 precipitation (dry and wet winters are equally likely; $S_+ = 1$).

This asymmetry in NM4 predictability is reversed in the later, post-1977 data subset (Fig. 5b). After 1977, when the PDO is generally positive (Fig. 1a), the set of five cold Niño-3 values leads to an insignificantly skewed precipitation distribution (1/2/2; $S_- = 1.2$) whereas warm Niño-3 values systematically lead to positive NM4 winter precipitation anomalies (1/0/6; $S_+ = 0.29$, with a 52% enhanced predictability of a wet winter).

Figures 6 and 7 illustrate the Niño-3-based S scores for all divisions in Arizona and New Mexico, with the data divided into pre-PDO-shift and post-PDO-shift years. The smaller numbers of years contained in each subsample lead to greater sampling uncertainty in each score relative to the statistics derived from the entire dataset, but the pronounced asymmetry in skewness in the two groups of years is readily apparent. In the pre-

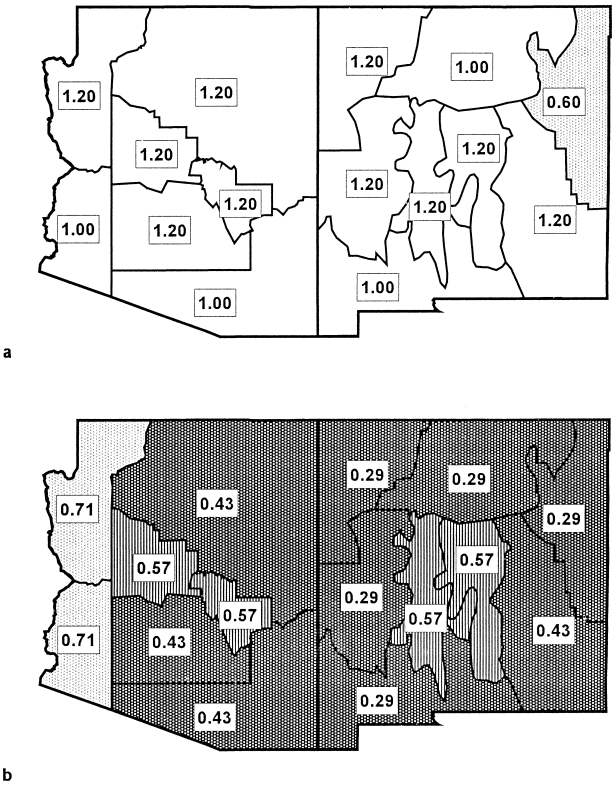

FIG. 7. As in Fig. 6 but based only on years after the 1977 PDO regime shift shown in Fig. 1a.

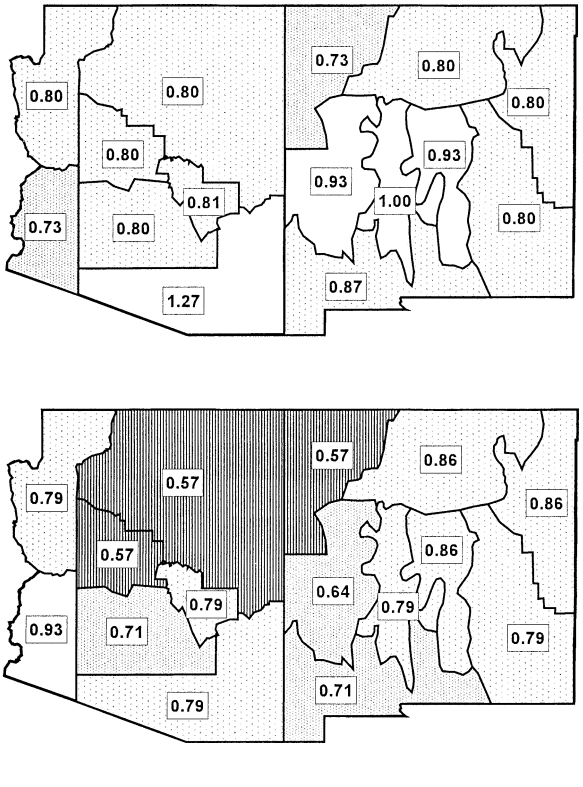

FIG. 8. (a) As in Fig. 4a but based only on years prior to the 1977 PDO regime shift shown in Fig. 1a. (b) As in Fig. 4b but based only on years after the 1977 PDO regime shift.

PDO-shift data (before 1977, when PDO was primarily negative) S_- scores associated with cold Niño-3 years (Fig. 6a) are smaller (more skill) than the corresponding values derived from the entire period of record (Fig. 3a) in every division except AZ7 (southeastern Arizona) and NM3 (New Mexico northeastern plains). On the other hand, seasonal predictability associated with warm Niño-3 is markedly worse in most divisions (Fig. 6b). Ten of 15 divisions in these two states exhibit S_+ scores above 0.9 in this subperiod, indicating that predictability during El Niño winters was practically nonexistent during these decades.

In the post-PDO-shift subset of years (1977–97) the asymmetry in ENSO-based predictability reverses across the Southwest. The small set of five cold Niño-3 years yields S_- scores greater than or equal to unity in 14 of 15 divisions (Fig. 7a). However the set of seven warm Niño-3 years exhibits a dramatic shift toward wet winters (Fig. 7b), with S_+ scores that are less than 0.75 in every division and less than 0.6 everywhere except the two westernmost divisions in Arizona.

Skill scores associated with PDO variability within the preshift and postshift data subsets (Fig. 8) are generally slightly lower than the analogous overall PDO-based scores (Fig. 4) but are much less impressive than the preshift and postshift Niño-3-based scores. In the 27 preshift years prior to 1977 there is only one upper-tercile PDO value, so only statistics associated with lower-tercile extrema are meaningful (Fig. 8a). Skill scores are less than 0.75 in only 2 of the 15 divisions in Arizona and New Mexico. When comparing Fig. 8a with Fig. 6a, it is seen that Niño-3 again provides more information than the PDO for prediction of dry winters.

The same comparisons hold for positive PDO as a predictor in the postshift decades. The postshift PDO-based S_+ scores in Fig. 8b are mostly a small amount lower than the S_+ scores based on PDO for the entire dataset (Fig. 4b); six divisions in Fig. 8b have scores less than 0.75. The PDO-based scores throughout the Southwest are not nearly as low as the Niño-3-based scores in Fig. 7b, however.

In summary, pronounced decadal variability in the predictive skill associated with ENSO SST is associated with the regime shift in 1977. Before the shift, cold Niño-3 temperature in late summer was an excellent predictor of a dry winter across the Southwest, but warm Niño-3 anomalies did not provide much predictive skill for subsequent winter precipitation. After the shift, warm Niño-3 values systematically led to wet winters but cold Niño-3 values were not of much use. Both before and after the shift, Niño-3 is a better interannual predictor of Southwest precipitation anomalies than are the interannual PDO fluctuations.

5. Discussion and conclusions

The goal of this study has been to clarify the seasonal statistical predictability of winter seasonal anomalies of precipitation in Arizona and New Mexico derived from antecedent knowledge of Pacific SST anomalies along the equator and in the North Pacific. Autumn-season (JAS) Niño-3 SST and the annually averaged Mantua et al. (1997) PDO index were used to characterize Pacific SST prior to each winter season. Predictability was assessed using a modified Brier score [Eq. (1)] that conveniently encapsulates the skewed three-bin precipitation distributions used operationally to describe probabilistic seasonal anomaly forecasts. The 48-yr period of record was initially considered as a single dataset. The ENSO cycle provided more predictability than the PDO index, and the ENSO-based seasonal predictability was modified only modestly by multivariate consideration of the PDO.

Using the PDO regime shift in 1977, the empirical predictability statistics were recalculated after splitting the data into preshift and postshift subsets. The statistics calculated on the partitioned data illustrated dramatic differences in ENSO-based predictive skill in the two subsets. During the pre-1977 period, when the PDO was largely negative, predictive skill was higher for cold Niño-3 temperatures leading dry winters in the Southwest than for warm Niño-3 leading wet winters; that is, La Niña provided a better basis for a winter seasonal forecast than El Niño did. After the regime shift in 1977, the asymmetry in predictability reversed, and El Niño was a better basis for a seasonal forecast than was La Niña. This single regime shift probably is responsible for most of the large effect of the PDO on seasonal climate anomalies that was documented by Gershunov and Barnett (1998) and Higgins et al. (2000). Echoing a principal conclusion in those two papers, and the McCabe and Dettinger (1999) study, the results presented here emphasize the importance for seasonal climate prediction of incorporating information about the phase of the PDO when formulating ENSO-based winter forecasts.

The PDO exhibits interannual variability in addition to the 1977 regime shift, however. Within both the pre-1977 and post-1977 subsets, fluctuations of the PDO only modestly affect the anomaly distribution of subsequent Southwest wintertime precipitation as compared with the predictability associated with Niño-3.

These results have several implications for operational seasonal forecasting. First, the practical utility of the PDO for seasonal forecasting is limited to some extent, because in real time it is difficult to distinguish a long-term regime shift (which apparently occurred just once in our 48-yr data record) from a shorter-timescale fluctuation. Thus, even if the PDO regime shift had been identified in 1977, the importance of that shift relative to other fluctuations (e.g., PDO variations in 1958 or 1991 in Fig. 1a) could not have been identified for the purposes of a seasonal forecast.

In this regard, the possibility that the PDO shifted regimes back into a negative phase in the late 1990s adds uncertainty to ENSO-based seasonal forecasts for the next few years. If the PDO has now returned to a long-term negative phase, then the very high ENSO-based predictability of wet winters in recent decades (Fig. 7b) may weaken, and instead the cold phase of ENSO will generate better predictability, as occurred before 1977 (Fig. 6a).

A second implication is somewhat more speculative, that is, whether North Pacific Ocean temperatures are truly responsible for the shift in ENSO-based predictability that unquestionably seems to have occurred in the late 1970s. On physical grounds it is unclear why short-term, year-to-year fluctuations of North Pacific SST should have any less influence on winter-season precipitation in the Southwest than multidecadal SST fluctuations do. However most of the PDO influence seems to be related to just one pronounced regime shift, because PDO-based interannual predictability within each regime is modest (Fig. 8).

Furthermore, studies of North Pacific SST variability identify other ''regime shifts'' that do not have effects on Southwest precipitation as pronounced as those of the 1977 shift. For example, Chao et al. (2000) point to 1957–58 as the year of another interdecadal Pacific SST regime shift in the latter half of the twentieth century. A shift in that year is difficult to see in Fig. 1a, and there is no obvious ENSO predictability change associated with that year. Perhaps some related component of the climate system that shifted in the late 1970s is the physical agent responsible for the different effect of ENSO fluctuations on southwest North American climate before and after 1977. Support for this possibility is found in a recent study by Pierce (2002), who found that specifying North Pacific SSTs in a coupled model did not force the circulation changes associated with observed decadal modulations of ENSO teleconnections.

The foregoing speculation cannot be addressed in our empirical study and probably cannot be resolved through purely empirical analyses of any kind. Better fundamental understanding of the dynamics of storm tracks and tropical–extratropical interactions will be required to make progress on this problem. Improvements in characterization and understanding of the PDO, including extending a record of its variability backward in time (Biondi et al. 2001), are necessary to define the PDO's far-field effects on climate. Meanwhile, even in the absence of dynamical understanding, it is appropriate to consider the asymmetry in ENSO-based seasonal predictability between the low-PDO and high-PDO climate regimes we have documented here.

Acknowledgments. Research by DSG and CT has been supported by grants from the U.S. National Science

Foundation (Award 97-31089) and the NOAA Office of Global Programs (Award NA06GP0377). Constructive reviews by C. Ropelewski, R. Cerveny, and K. Redmond led to significant improvements in the manuscript.

REFERENCES

Barlow, M., S. Nigam, and E. H. Berbery, 2001: ENSO, Pacific decadal variability, and U.S. summertime precipitation, drought, and stream flow. *J. Climate,* **14,** 2105–2108.

Bernal, G., P. Ripa, and J. C. Herguera, 2001: Variabilidad oceanográfica y climática en el bajo Golfo de California: Influencias del trópico y Pacífico Norte (Oceanographic and climatic variability in the lower Gulf of California: Influences of the Tropics and the North Pacific). *Cien. Mar.,* **27,** 595–617.

Biondi, F., A. Gershunov, and D. R. Cayan, 2001: North Pacific decadal climate variability since 1661. *J. Climate,* **14,** 5–10.

Brito-Castillo, L., A. Leyva-Contreras, A. V. Douglas, and D. Lluch-Belda, 2002: Pacific decadal oscillation and the filled capacity of dams on the rivers of the Gulf of California continental watershed. *Atmósfera,* **15,** 121–138.

Cayan, D. R., and R. H. Webb, 1992: El Niño/Southern Oscillation and stream flow in the western United States. *El Niño: Historical and Paleoclimatic Aspects of the Southern Oscillation,* H. Diaz and V. Markgraf, Eds., Cambridge University Press, 29–68.

Chao, Y., M. Ghil, and J. C. McWilliams, 2000: Pacific interdecadal variability in this century's sea surface temperatures. *Geophys. Res. Lett.,* **27,** 2261–2264.

Deser, C., and J. M. Wallace, 1987: El Niño events and their relationship to the Southern Oscillation. *J. Geophys. Res.,* **92,** 14 189–14 196.

Gershunov, A., and T. P. Barnett, 1998: Interdecadal modulation of ENSO teleconnections. *Bull. Amer. Meteor. Soc.,* **79,** 2715–2725.

Graham, N. E., 1994: Decadal-scale climate variability in the tropical and North Pacific during the 1970s and 1980s: Observations and model results. *Climate Dyn.,* **10,** 135–162.

Gutzler, D. S., 1996: Low-frequency ocean–atmosphere variability across the tropical western Pacific. *J. Atmos. Sci.,* **53,** 2773–2785.

Higgins, R. W., A. Leetmaa, Y. Xue, and A. Barnston, 2000: Dominant factors influencing the seasonal predictability of U.S. precipitation and surface air temperature. *J. Climate,* **13,** 3994–4017.

Latif, M., and T. P. Barnett, 1994: Causes of decadal climate variability over the North Pacific and North America. *Science,* **266,** 634–637.

——, and ——, 1996: Decadal climate variability over the North Pacific and North America: Dynamics and predictability. *J. Climate,* **9,** 2407–2423.

Liles, C., 2000: Relationships between the Pacific decadal oscillation and New Mexico annual and seasonal precipitation. *Proc. Second Southwest Weather Symposium,* Tucson, AZ, NWS–University of Arizona–COMET, 7 pp.

Mantua, N. J., S. R. Hare, Y. Zhang, J. M. Wallace, and R. C. Francis, 1997: A Pacific interdecadal climate oscillation with impacts on salmon production. *Bull. Amer. Meteor. Soc.,* **78,** 1069–1079.

McCabe, G. J., and M. D. Dettinger, 1999: Decadal variations in the strength of ENSO teleconnections with precipitation in the western United States. *Int. J. Climatol.,* **19,** 1399–1410.

Molles, M. C., Jr., and C. N. Dahm, 1990: A perspective on El Niño and La Niña: Global implications for stream ecology. *J. N. Amer. Benthol. Soc.,* **9,** 68–76.

Pierce, D. W., 2002: The role of sea surface temperatures in interactions between ENSO and the North Pacific Oscillation. *J. Climate,* **15,** 1295–1308.

Rasmusson, E. M., and T. H. Carpenter, 1982: Variations in the tropical sea surface temperature and surface wind fields associated with the Southern Oscillation/El Niño. *Mon. Wea. Rev.,* **110,** 354–384.

Redmond, K. T., and R. W. Koch, 1991: Surface climate and stream flow variability in the western United States and their relationship to large-scale circulation indices. *Water Resour. Res.,* **27,** 2381–2399.

Ropelewski, C. F., and M. S. Halpert, 1986: North American precipitation and temperature patterns associated with the El Niño–Southern Oscillation (ENSO). *Mon. Wea. Rev.,* **114,** 2352–2362.

——, and ——, 1987: Global and regional scale precipitation patterns associated with the El Niño–Southern Oscillation. *Mon. Wea. Rev.,* **115,** 1606–1626.

Stephens, C., S. Levitus, J. Antonov, and T. P. Boyer, 2001: On the Pacific Ocean regime shift. *Geophys. Res. Lett.,* **28,** 3721–3724.

Thornbrugh, C., C. Liles, D. Kann, and D. Gutzler, 2001: Modulation of ENSO-related climate variations across the southwest U.S. by the Pacific decadal oscillation. Preprints, *Symp. on Climate Variability, the Oceans, and Societal Impacts,* Albuquerque, NM, Amer. Meteor. Soc., 222–224.

Trenberth, K. E., 1997: Short-term climate variations: Recent accomplishments and issues for future progress. *Bull. Amer. Meteor. Soc.,* **78,** 1081–1096.

——, G. W. Branstator, D. Karoly, A. Kumar, N.-C. Lau, and C. Ropelewski, 1998: Progress during TOGA in understanding and modeling global teleconnections associated with tropical sea surface temperatures. *J. Geophys. Res.,* **103,** 14 291–14 324.

Wallace, J. M., E. M. Rasmussen, T. P. Mitchell, V. E. Kousky, E. S. Sarachik, and H. von Storch, 1998: On the structure and evolution of ENSO-related climate variability in the tropical Pacific: Lessons from TOGA. *J. Geophys. Res.,* **103,** 14 241–14 260.

Weare, B. C., A. R. Navato, and R. E. Newell, 1976: Empirical orthogonal function analysis of Pacific sea surface temperatures. *J. Phys. Oceanogr.,* **6,** 671–678.

Wilks, D. S., 1995: *Statistical Methods in the Atmospheric Sciences.* Academic Press, 467 pp.

Zhang, Y., J. M. Wallace, and D. S. Battisti, 1997: ENSO-like interdecadal variability: 1900–93. *J. Climate,* **10,** 1004–1020.